Lymphology 38 (2005) 50-65

HYALURONAN AND SULPHATED HYALURONAN MICROPATTERNS: EFFECT OF CHEMICAL AND TOPOGRAPHIC CUES ON LYMPHATIC ENDOTHELIAL CELL ALIGNMENT AND PROLIFERATION

D. Pasqui, A. Rossi, R. Barbucci, S. Lamponi, R. Gerli, E. Weber

Department of Neuroscience (AR,RG,EW), Molecular Medicine Section and Department of Chemical and Biosystem Science and Technology (DP,RB,SL), University of Siena, Siena, Italy; Interuniversity Research Center for Advanced Medical Systems (DP,AR,RB,SL,EW); DP and AR contributed equally to this work.

ABSTRACT

While tissue engineered blood vessels have entered surgical practice, the construction of artificial lymphatic vessels has never been attempted due to the small dimensions and fragility of lymphatic vessels. A possible alternative would be to obtain a new growth of interrupted lymphatic vessels. We have previously reported that lymphatic endothelial cells align when cultured on striped micropatterns of hyaluronan (Hyal) and aminosilanized glass. We here report a comparative study in which lymphatic endothelial cells have been plated on micropatterns with stripes of different width and height obtained by the photoimmobilization of Hyal and its sulphated derivative (HyalS) on aminosilanized glass to verify whether their response correlated with surface-chemistry and/or topography. On Hyal micropatterns, cells adhered to aminosilanized glass, avoiding Hyal stripes and molding their shape in accordance to the micropattern topography. Stress fibers, integrins and focal adhesion kinase organized accordingly. HyalS micropatterns with the same topography were unable to guide cell response, cells randomly adhered to HyalS and glass stripes, and polarization was attained only by increasing stripe height. These data indicate that surface chemistry is the main cue responsible for lymphatic endothelial cell guidance. When surface chemistry of stripes promotes cell adhesion as well as that of the substrate, topographical parameters become prevalent. Micropatterns with defined chemical and topographical properties may contribute to the design of new platforms for controlled cell growth in tissue engineering of lymphatic vessels.

After lengthy experimentation in vitro and in animal models (1), tissue engineered blood vessels have entered surgical practice and have proved of great value particularly in pediatric patients for their capability to remodel during childhood growth (2,3). The construction of an artificial lymphatic vessel mimicking a real one is hampered by small dimensions and fragility of the wall, which would render its manipulation and insertion into the recipient a challenge. In our opinion, a more practicable strategy would be to reconstruct interrupted lymphatic routes by guiding the new growth of adjacent lymphatic vessels. We have previously reported that microstructured surfaces containing geometrically defined bio-adhesive and non-adhesive domains, i.e., alternating stripes of aminosilanized glass and Hyaluronan (Hyal),

are effective in attaining the alignment and growth of cultured lymphatic endothelial cells in the desired direction (4).

We here report a comparative study in which lymphatic endothelial cells have been plated on micropatterned surfaces with stripes of different width (from 50 to 5µm) and height (from 35 to 250nm) obtained by the photoimmobilization of Hyal and its sulphated derivative HyalS on aminosilanized glass in order to understand whether the response of lymphatic endothelial cells correlated with surface-chemistry and/or topography. Cell behavior on unpatterned surfaces of the same polysaccharides was also evaluated.

Hyal is a high molecular weight polysaccharide made of alternating N-acetyl-D-glucosamine and ß-D-glucuronic acid residues. It is highly hydrophilic because of its large number of hydroxyl and carboxyl groups. Hyal is one of the glycosaminoglycan components of the extracellular matrix (5-7). It is produced at the plasma membrane level by Hyal synthetase and extruded from the cell (8). Its synthesis increases during cell migration (9), mitosis (10), and cancer invasion (11). Hyal binds to cells by direct interaction with cell surface receptors (12). The cell-signaling function is mediated by CD44 receptor in blood (13) and LYVE-1 in lymphatic endothelial cells (14).

Purified Hyal has been employed as a structural material in tissue engineering because of its high molecular weight and capability to form tridimensional networks. The properties of this macromolecule may be molded by chemical modifications. One of the most interesting is the insertion of sulphate groups on the hydroxilic groups of the polysaccharide, which gives the macromolecule heparin-like activity. In this work, a HyalS polymer containing about 3.5 sulphate groups for each repeat unit, which has been demonstrated to provide the greatest anticoagulant properties (15), has been used.

Very little information is available on the biological activity on cell behavior of HyalS or other sulphated glycosaminoglycans. Most of the data concern their antithrombotic effect (16), which is not as relevant in lymphatic as in blood vessels.

We have investigated how the different chemistry of Hyal and HyalS affects lymphatic endothelial cell (LEC) behavior. The effect of surface topography has also been investigated. Surfaces with the same chemistry, but containing different topographical features, have been demonstrated to influence cell behavior in different ways affecting cell shape and functionality (17,18). Finally, we raise the question: is lymphatic endothelial cell behavior influenced more by surface chemistry or topography?

MATERIALS AND METHODS

Polysaccharides

Hyaluronan sodium salt (MW 240000) was provided by Biophyl S.p.A. (Germany). Sulphated Hyaluronan was obtained by the insertion of sulphate groups in the oxidrilic groups of Hyal. The sulphation degree, which theoretically ranges from one to four, was controlled by varying the Hyal/sulphating agent molar ratio. The synthesis and the characteristics of HyalS have already been described (19). The HyalS polymer used in this study contained 3.5 sulphate groups.

Fabrication of Micropatterned Hyal and HyalS surfaces

Micropatterned surfaces with different chemical and topographical heterogeneities were obtained by photoimmobilization of Hyal and HyalS on silanized glass coverslips in the presence of a chromium-quartz photomask with features of defined dimensions and geometry. The polysaccharide works as a negative photoresist which, upon exposure to UV light, remains grafted to the surface. The whole process *(Fig. 1)* consists of the four following steps: 1) Conjugation of the polysaccharide (Hyal or HyalS) with a

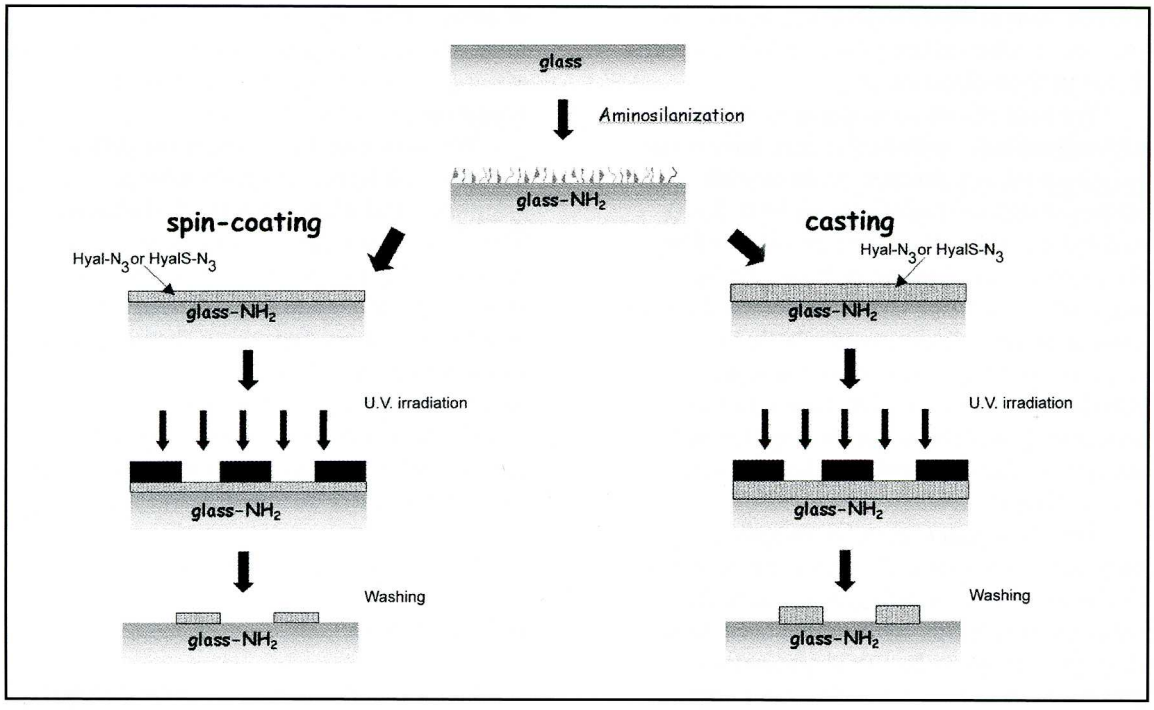

Fig. 1. Scheme of the photoimmobilization process by spin-coating (left) and casting (right). Note the different height of the polymer stripes obtained. Hyal-N_3 and HyalS-N_3 = Hyal and HyalS conjugated with azidoaniline.

photoreactive moiety (4-azido-aniline) to make it reactive to U.V. light (20). 2) Aminosilanization of the glass substrate (21). The silanized glass is hereafter referred to as glass-NH_2. 3) Deposition of the photoreactive polysaccharide solution on glass-NH_2 either by casting or spin-coating. In the casting procedure, a defined volume of a 0.1% w/v polysaccharide solution is deposited on the surface and allowed to dry in dark conditions. A thick, non-homogeneously distributed layer of polysaccharide is obtained. Environmental factors such as humidity and temperature affect the results. Spin-coating gives more reproducible results. Briefly, 50µl of a 1% w/v of aqueous polysaccharides is spin coated onto the surface at 2500 rpm for 30sec. 4) Photoimmobilization of the polysaccharide on the substrate by irradiation with a UV light in the presence of a chromium-quartz photomask containing stripes of different dimensions (50, 25 and 5µm wide) followed by washing with double distilled water to remove any unbound polysaccharide. Homogeneous, unpatterned Hyal or HyalS surfaces were realized with the same procedure without using the photomask.

Surface Topography and Chemistry

Hyal and HyalS micropatterns were analyzed by Atomic Force Microscope (AFM Thermo Microscope, Veeco Instruments, France). AFM images were obtained in different areas of the samples by operating in non-contact mode in air, using a silicon tip. Surface roughness was measured in 5x5µm^2 scans with the help of SPLM-Lab version 5.01 software.

Lymphatic Endothelial Cells

LEC were obtained from bovine thoracic

duct by collagenase treatment as previously described (22) and cultured in DMEM with 20% Fetal Bovine Serum (FBS), 2mM glutamine, 100µg/ml endothelial cell growth supplement and 50µg/ml gentamycin. At confluence, cells were trypsinized, resuspended in DMEM with 10% FBS and gentamycin and seeded at the density of $1.5x10^4$ cells/100µl onto each of the following ethanol sterilized samples:

- micropatterns of Hyal or HyalS (obtained by spin-coating or casting) on glass-NH_2 coverslips
- unpatterned Hyal or HyalS on glass-NH_2 coverslips
- glass-NH_2 coverslips.

Once the cells had adhered to the surface, 900µl of medium was added.

Identification of Cells by Acetylated LDL Uptake

Cells were identified as endothelial by their capacity to uptake and internalize acetylated low density lipoproteins labeled with a fluorescent probe, 1,1'-dioctadecyl-3,3,3'3'-tetramethylindo-carbocyanine perchlorate (Dil-Ac-LDL, Biomedical Technologies Inc, Stoughton, MA, USA) (23) according to the manufacturer's instructions. Nuclei were counterstained with Hoechst.

Double Labeling of Integrins and Focal Adhesion Kinase

Immunohistochemical studies were performed on cells cultured on Hyal/glass-NH_2 micropatterns and on HyalS/glass-NH_2 obtained by spin-coating but not by casting because the latter tended to detach during the numerous passages of the double labeling procedure.

Cells were fixed with cold acetone for 10 min. at -20°C, washed with Phosphate Buffered Saline (PBS) containing 0.5% Bovine Serum Albumin (BSA, Sigma) and 0.1% Triton-X-100 (hereafter referred to as buffer) and permeabilized for 40 min. with PBS containing 0.1% Triton and 3% BSA to block unspecific binding sites. Cells were then incubated overnight at 4°C with a polyclonal antibody to α-v integrins (Chemicon) diluted 1:15 in buffer, washed and incubated with a FITC conjugated goat anti-rabbit secondary antibody for 2h. Prior to the second labeling, unspecific binding sites were again blocked with PBS containing 3% BSA and 5% goat serum for 40 min. Cells were then incubated with a monoclonal antibody to focal adhesion kinase (FAK, Chemicon) diluted 1:20 in buffer for 2h. After washing, cells were incubated with a TRITC conjugated secondary antibody for 2h. Coverslips were mounted upside down with DABCO (Sigma) and viewed with a Nikon ECLIPSE E600 fluorescence microscope.

ß-actin Staining

ß-actin, a typical cytoskeletal protein of endothelial cells, was evaluated in LEC cultured on Hyal/glass-NH_2 and HyalS/glass-NH2 micropatterns obtained by spin-coating. It was stained with phalloidin-FITC (Sigma) according to the manufacturer's instructions following fixation with formalin and permeabilization with Triton. Double labeling of actin (stained with phalloidin-TRITC) and αv integrins was performed on LEC cultured on Hyal/glass-NH_2 micropatterns.

Cell Counts

To evaluate whether lymphatic endothelial cells preferentially adhered to HyalS or to glass-NH_2, the number of adherent cells was determined under phase contrast microscopy with a 16x objective at different times of culture (4, 24, 48 hours). Cells were counted in 5 randomly selected photographic fields/sample (0.47mm^2 each). Three samples were counted for each experimental condition, and each experiment was repeated at least three times.

Statistical analysis was performed using Microcal™ Origin® (Microcal Software, Inc.

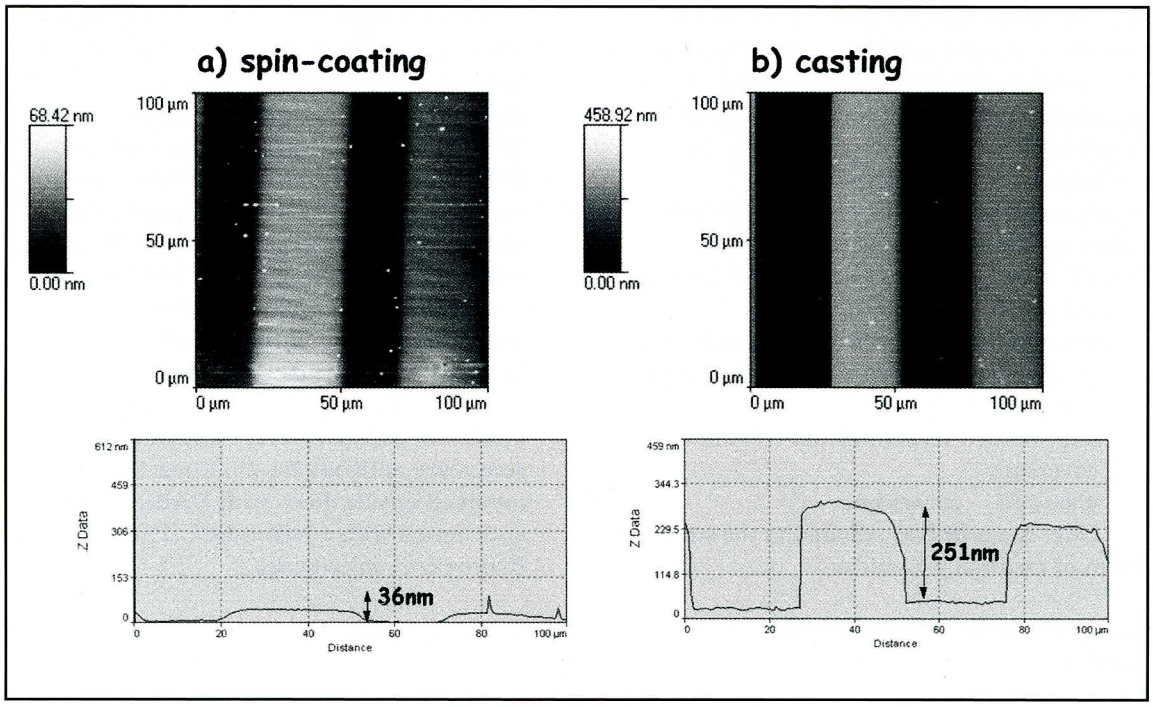

Fig. 2. AFM scans of HyalS micropatterns with stripes of 25µm obtained by: a) spin-coating and b) casting. The different height of stripes is shown in the section profile (bottom).

Northampton, Massachusetts, USA). The significance of the reported means was determined using the two population t-test comparing each sample type with the two control surfaces (glass-NH_2 and unpatterned polysaccharides). Data were expressed as mean±standard error (SE).

SEM Analysis

Micropatterned surfaces were fixed with 2.5% glutaraldehyde, dehydrated in ethanol, desiccated overnight, gold sputtered with an automatic sputter coater (BAL-TEC SCD 050, Balzers, Germany) and then observed by scanning electron microscopy (SEM) (XL20 Philips, The Netherlands) operating at 15kV.

RESULTS

Surface Topography and Chemistry

AFM was used to check the surface topography of Hyal and HyalS micro-patterned surfaces. *Fig. 2* shows AFM scans of HyalS micropatterns with 25µm wide stripes obtained by spin-coating and casting. The stripes were easily visible, and their width and separating space corresponded to the dimensions of the mask used in the photoimmobilization. The edge of the stripes was not sharp, and rather showed a gentle slope of a few nanometers due to the softness and mobility of the polysaccharide. The step height was about 30nm for Hyal and HyalS patterns prepared by spin-coating and about 200-250nm for polysaccharide patterns prepared by casting.

The top part of the stripes was smooth, with mean roughness values Ra of 3.30 ± 0.75nm for Hyal stripes and of 4.10 ± 0.74nm for HyalS ones in a dry state. Upon exposure to water, surface roughness of Hyal and

Fig. 3. Light micrographs of LEC stained with Giemsa 48h after seeding. LEC adhere to glass-NH_2 (a) and unpatterned HyalS (c), but not to unpatterned Hyal (b). Orig.mag. x10.

HyalS increased to 5.95 ± 0.51 and 6.3 ± 0.65nm respectively while that of glass-NH_2 did not vary (data not shown).

ToF-SIMS imaging demonstrated a good surface chemical contrast between Hyal or HyalS and the glass domains as previously reported (24); thus a micropatterned polysaccharide surface with a defined chemical pattern has been obtained.

Pattern Stability

AFM analysis showed that when the micropatterns were kept in culture medium for a week, no changes either in the morphology or dimensions occurred in the thinner stripes prepared by spin-coating, whereas polysaccharide swelling with widening and thickening of the stripes and eventually detachment from the substrate was observed in the thicker patterns prepared by casting.

Unpatterned Hyal and HyalS Surfaces: Same Topography, Different Surface Chemistries

Unpatterned layers of Hyal and HyalS have been utilized to evaluate the effect of surface chemistry on cell behavior. LEC rapidly adhered to and proliferated well on HyalS layers just as on glass-NH_2 *(Fig. 3)*. Conversely, no adhesion was found on photoimmobilized Hyal surfaces even after 7 days of culture. Considering that surface roughness in wet conditions is more or less the same, surface chemistry due to the introduction of sulphated groups might be responsible for cell response.

Hyal and HyalS Micropatterns

LEC plated on Hyal micropatterned substrates avoided the Hyal domains and adhered only to the glass-NH_2 ones as previously reported (4). Cell growth was guided along the micropattern direction: cells assumed an elongated shape and polarized along the main longitudinal axis of the stripe *(Fig. 4)*. They arranged in 3-4 parallel rows in 50µm wide stripes, in 2 rows in 25µm wide stripes, in a single row in 5µm wide stripes. With insufficient space to spread in 5µm wide stripes, LEC remained elongated, packed and prominent *(Fig. 4c)*. They often came in contact with neighboring cells in the adjacent stripe forming groups bridging more than one stripe. This behavior was particularly evident when the culture time was protracted for several days.

LEC cultured on HyalS/glass-NH_2 micropatterns obtained by spin-coating were not guided by the surface patterns and randomly distributed both on glass-NH_2 and polysaccharide domains with a polygonal flat shape *(Fig. 4d, e and f)* without any polarization. No significant influence of the stripes step was revealed; cells passed over

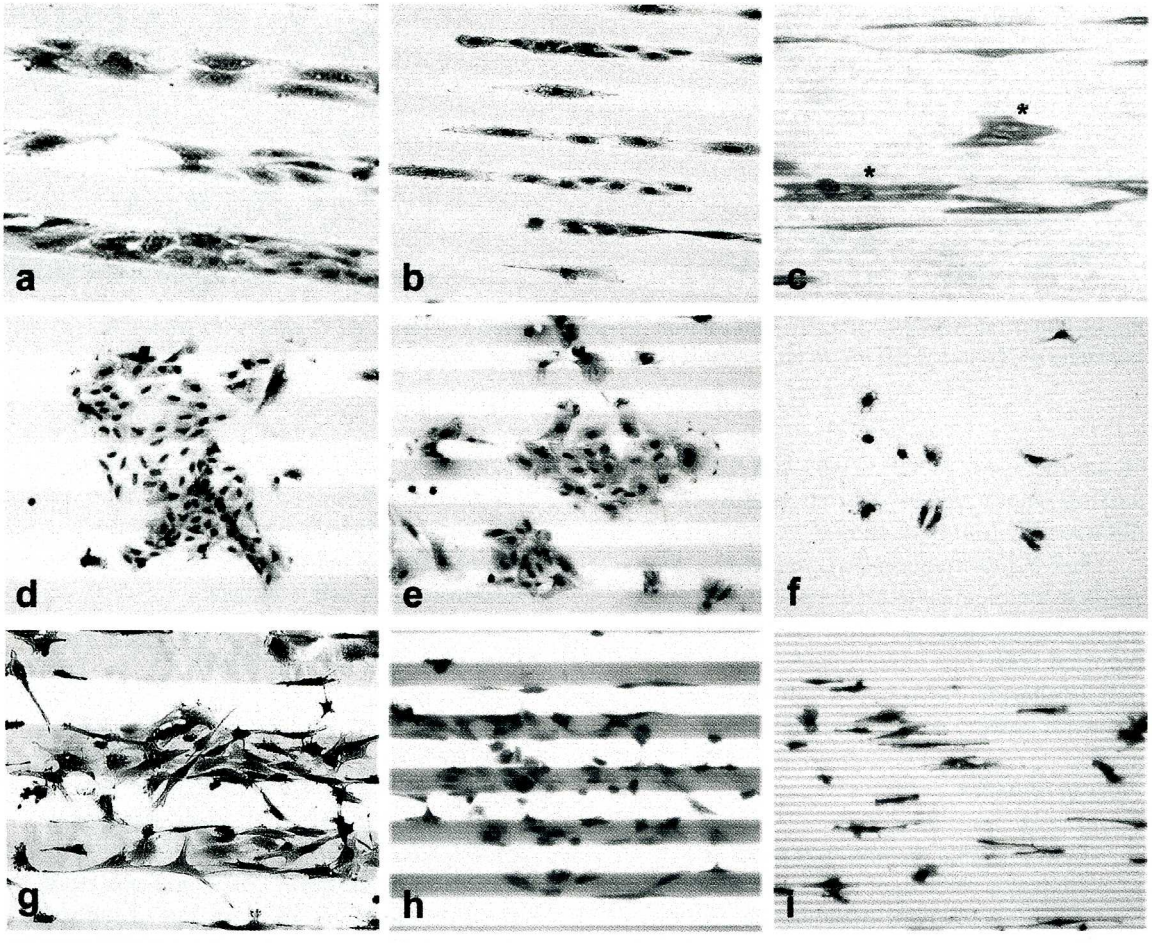

Fig. 4. Light micrographs of LEC stained with Giemsa 48h after seeding. LEC adhering to Hyal micropatterns (a-c), HyalS micropatterns obtained by spin-coating (d-f) and HyalS micropatterns obtained by casting (g-i) with stripes 50 (a, d, g), 25 (b, e, h) and 5 (c, f, i) μm wide. On Hyal micropatterns with wide stripes (a-b) LEC exclusively adhere to the glass-NH_2 domains avoiding the polymer and align parallel to the stripes; on 5 μm Hyal micropatterns (c) all cells align along the stripes but some form groups extending over several stripes (asterisks), others arrange in rows on glass-NH_2 stripes. On HyalS micropatterns obtained by spin-coating (d-f), LEC do not align and are randomly scattered on the polymer and on glass-NH_2 .On HyalS micropatterns obtained by casting (g-i), most of LEC preferentially adhere to the polymer and some align on the stripes edges. Orig. mag. x20.

the stripes step, perfectly adhering to them. On wider stripes, cells sometimes aggregated in colonies covering several adjacent stripes.

In order to investigate whether HyalS micropatterns with a higher thickness were able to affect cell response, HyalS micro-stripes with the same width were prepared by casting. Following this procedure, microstripes with a step height ranging from 200 to 250nm were obtained. After 24h of culture, cells preferentially adhered to the stripe edge and started to elongate along it. The most remarkable effect was noticed on 25μm wide stripes where many round cells first adhered to the edge and eventually polarized along the stripe direction *(Fig. 4h)*. After 48h of culture, many cells were still polarized along stripe edges, but several others moved towards polysaccharide domains and spread on them as shown in

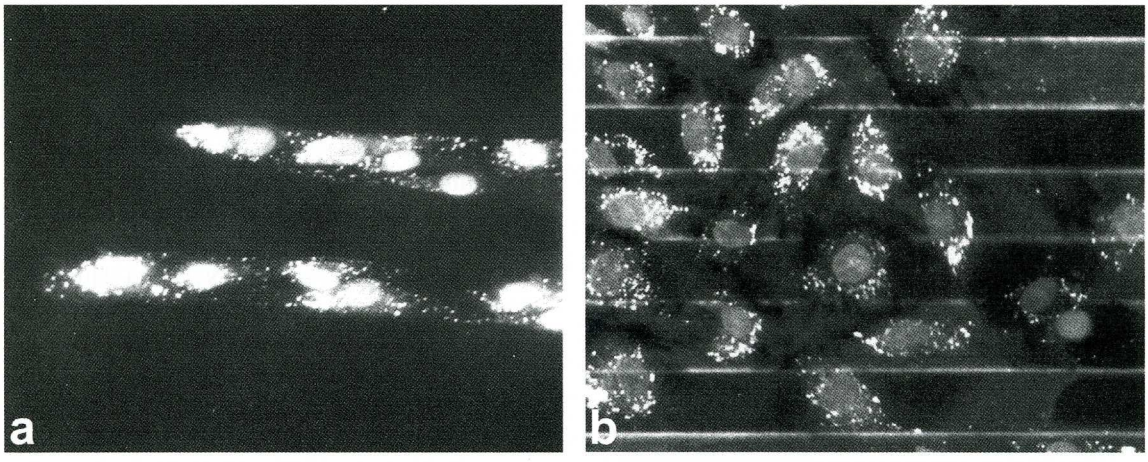

Fig. 5. DiI-Ac LDL uptake by LEC cultured on Hyal (a) and HyalS (b) micropatterns with 25µm wide stripes. Nuclei Hoechst counterstaining shows that all cells are positive for this endothelial marker. Orig. mag. x40.

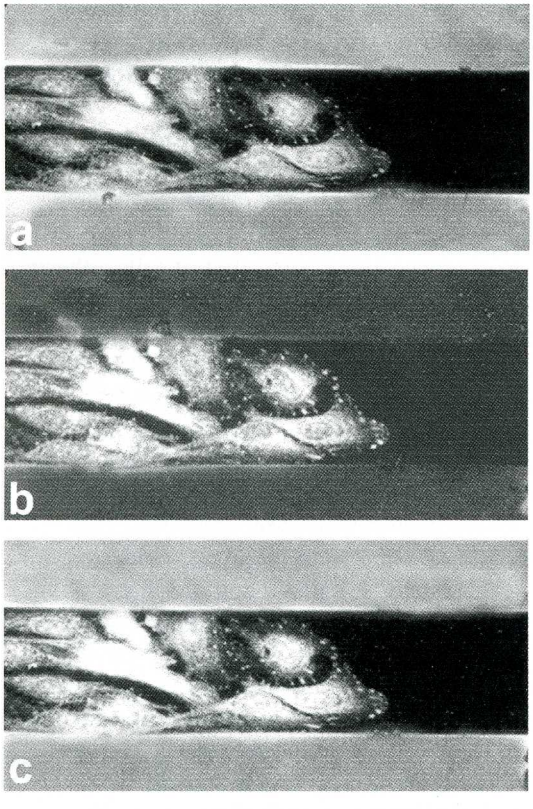

Fig. 6. Double labeling of α-v integrins and FAK in LEC cultured on Hyal/glass-NH2 micropatterns with 25µm wide stripes. Integrins (a) and FAK (b) co-localize along cell borders and at the leading edge of migrating cells as shown by merge (c).Orig. mag. x40.

50µm wide stripes *(Fig. 4g)*. On 5µm striped surfaces *(Fig. 4i)*, cells were very sensitive to the surface topography: in fact, most cells lined up along the stripes, and some spread with a flattened star-like morphology due to several pseudopodia which branched out from the cell body sticking on the stripe edge.

Acetylated LDL Staining

LEC cultured on Hyal or HyalS micropatterns stained brightly and uniformly with DiI-Ac-LDL *(Fig. 5)*. Acetylated LDL appeared as a punctate red fluorescence in the cytoplasm particularly around the nucleus. Nuclear Hoechst counterstaining demonstrated that virtually all cells were positive for this endothelial marker.

Immunostaining of Integrins and Focal Adhesion Kinase

The distribution of α-v integrins and FAK in LEC cultured on Hyal micropatterns with 50µm wide stripes is shown in *Fig. 6*. The fluorescent dashes of integrin clusters and FAK co-localized along cell borders of isolated cells, at the leading edge of migrating cells and where cells came in contact with each other, all probable sites of focal adhesion

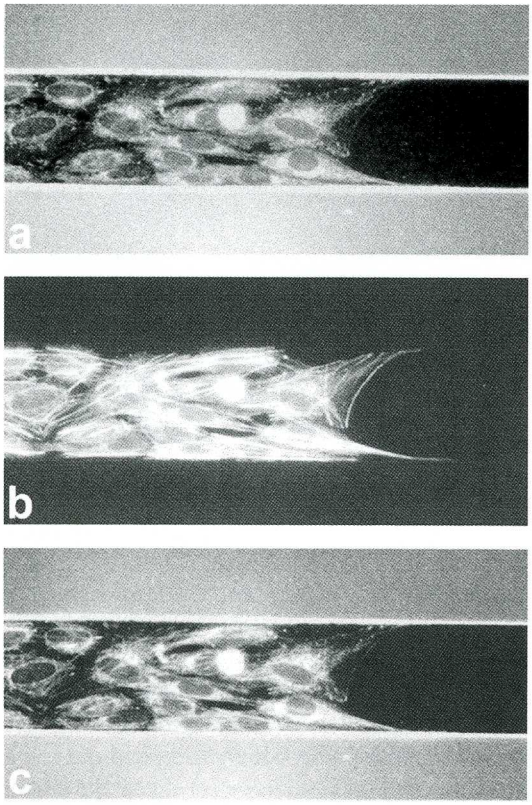

Fig. 7. Double labeling of α-v integrins (a) and ß-actin (b) in LEC cultured on Hyal/glass-NH_2 micropatterns with 25µm wide stripes. Actin stress fibers terminations on cell membrane correspond to integrin dashes (c) which apparently condition their orientation. Orig. mag. x40.

formation. Double staining for αv integrin and ß-actin *(Fig. 7)* indicated that integrin dashes were localized at the end of actin fibers.

ß-actin staining

ß-actin staining was performed on cells cultured on micropatterns with 25 and 5mm wide stripes. On Hyal micropatterns, actin fibers arranged in bundles parallel to the stripe direction *(Fig. 8a and c)* whereas on HyalS micropatterns, they did not sense the topography *(Fig. 8b and d)*, and their organization did not differ from that of cells grown on unpatterned glass-NH_2.

Cell Number

The number of adhering cells was evaluated after 4, 24 and 48h of culture on unpatterned glass-NH_2, unpatterned HyalS and micropatterned HyalS/glass-NH_2 surfaces obtained by spin-coating and casting, to ascertain whether cells preferentially adhered to HyalS or glass-NH_2 and which surface better promoted their proliferation. No cells were ever detected on Hyal stripes.

Cell counts on unpatterned HyalS surfaces compared with unpatterned glass-NH_2 substrates are reported in *Fig. 9*. On unpatterned glass-NH_2 substrates, cell number rapidly increased in the first 24h, remaining constant thereafter. On unpatterned HyalS surfaces, cell number increased with time with a different trend: gradually on surfaces obtained by spin-coating, rapidly from 24 to 48h on those obtained by casting.

Cell number on micropatterned surfaces of wide dimensions is reported in *Fig. 10*. The number of cells adhering inside the thinner HyalS microdomains obtained by spin-coating was higher than that of cells adhering on the thicker stripes of the same polysaccharide obtained by casting. Taking into consideration that the area covered by HyalS is the same for both surfaces, there is no apparent reason for such a great difference in cell number. On micropatterned surfaces of 50 µm obtained by spin-coating *(Fig. 10a)*, cell number increased on glass-NH_2 and HyalS domains with the same trend, and no cells aligned along the edge. On micropatterned surfaces of 50 µm obtained by casting, some cells lined up along the stripe edge and their number increased with time *(Fig. 10b)* while the number of cells adhering on glass-NH_2 domains decreased, and that of cells adhering on HyalS increased. This observation may signify either that cells moved from glass-NH_2 towards HyalS domains or that cell proliferation on HyalS was greater than on glass-NH_2. Overall cell adhesion was higher on surfaces obtained by

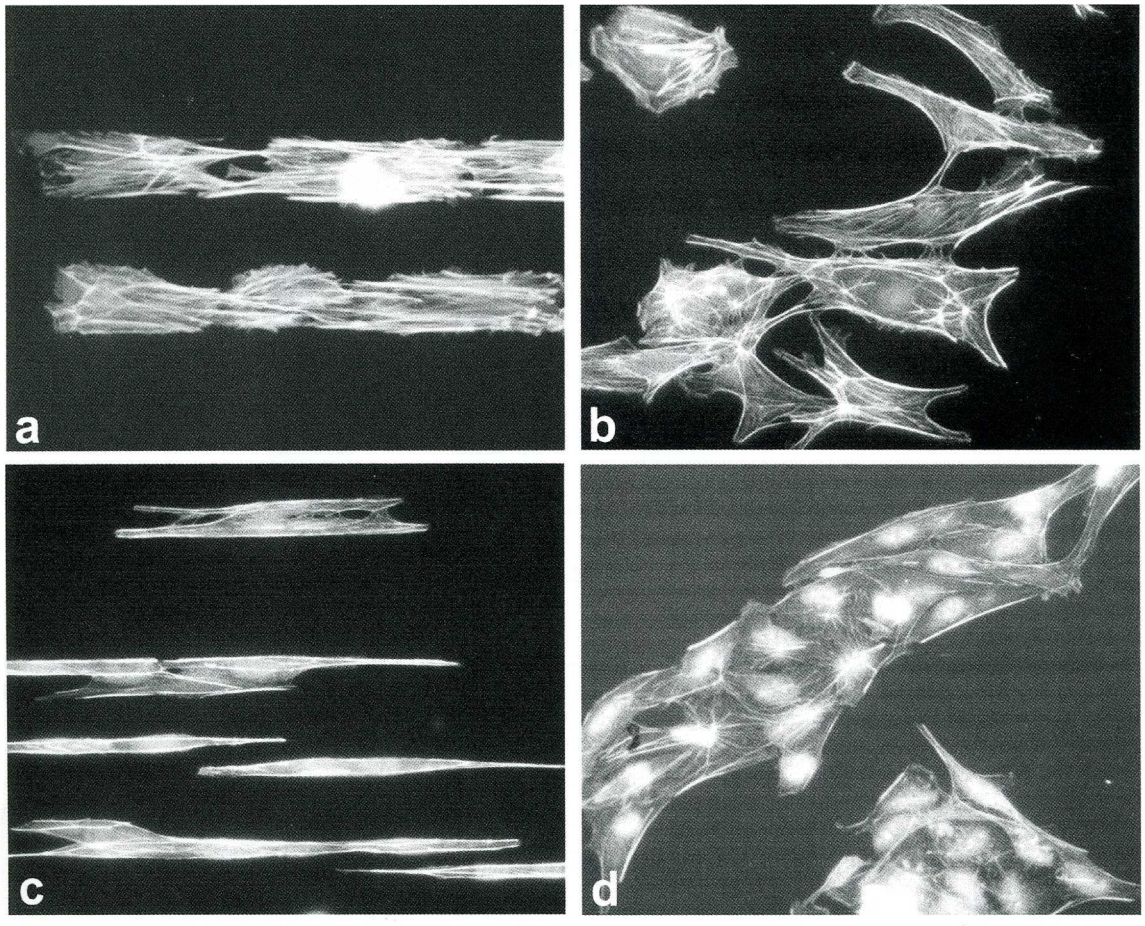

Fig. 8. ß-actin staining of LEC cultured on Hyal (a and c) and HyalS (b and d) micropatterns with 25 (a and b) and 5 (c and d) µm wide stripes. Actin stress fibers align parallel to the stripes on Hyal (a and c) but not on HyalS (b and d) micropatterns. Orig. mag. x40.

spin-coating, and cell proliferation was higher on surfaces obtained by casting.

On micropatterns consisting of stripes 5µm wide *(Fig. 11)*, it was not possible to distinguish cells adhering to HyalS from those adhering to glass stripes; accordingly, the parameter evaluated was the total number of aligned cells (irrespective of whether they adhered to HyalS or glass-NH_2) compared with the number of non-aligned cells. On micropatterned surfaces obtained by spin-coating *(Fig. 11a)*, only a small number of cells aligned and their number remained constant with time, whereas the number of non-aligned cells, which were the majority, increased with time. On micropatterns obtained by casting *(Fig. 11b)*, most cells lined up along the microstripes but their number did not increase significantly with time. The total number of adhering cells was much higher on micropatterned surfaces obtained by spin-coating than by casting. On micropatterns containing narrow stripes (i.e., 5µm), the topographical cue apparently played a key role in affecting cell behavior: thicker stripes (obtained by casting) were recognized by cells as an obstacle; accordingly, cell alignment was promoted and cell

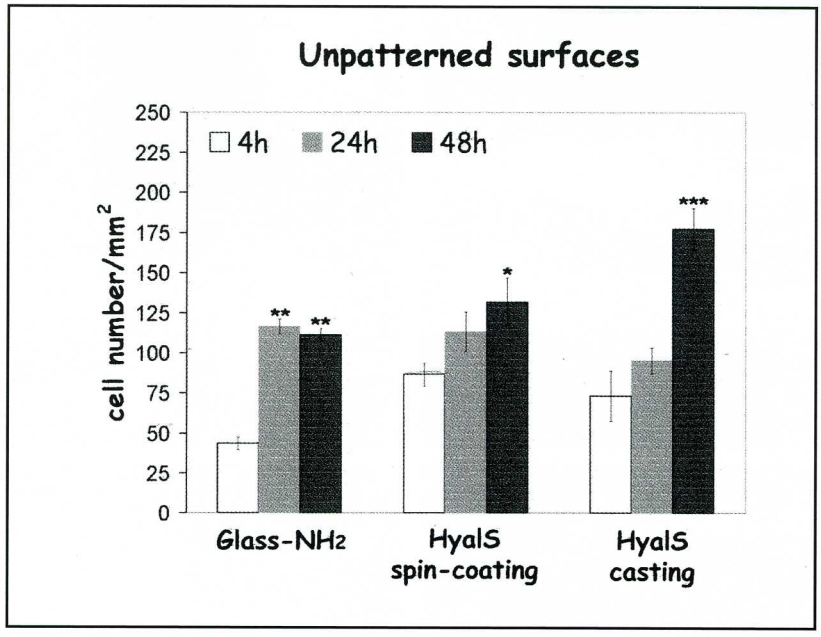

*Fig. 9. Number of adhering cells on unpatterned substrates (glass-NH_2, HyalS obtained by spin-coating and casting) at 4, 24 and 48h of culture. Cell number increases gradually on HyalS obtained by spin-coating and rapidly from 24 to 48h on HyalS obtained by casting. ***P< 0.001 vs 4 and 24 h, **P< 0.001 vs 4 h, *P< 0.05 vs 4h.*

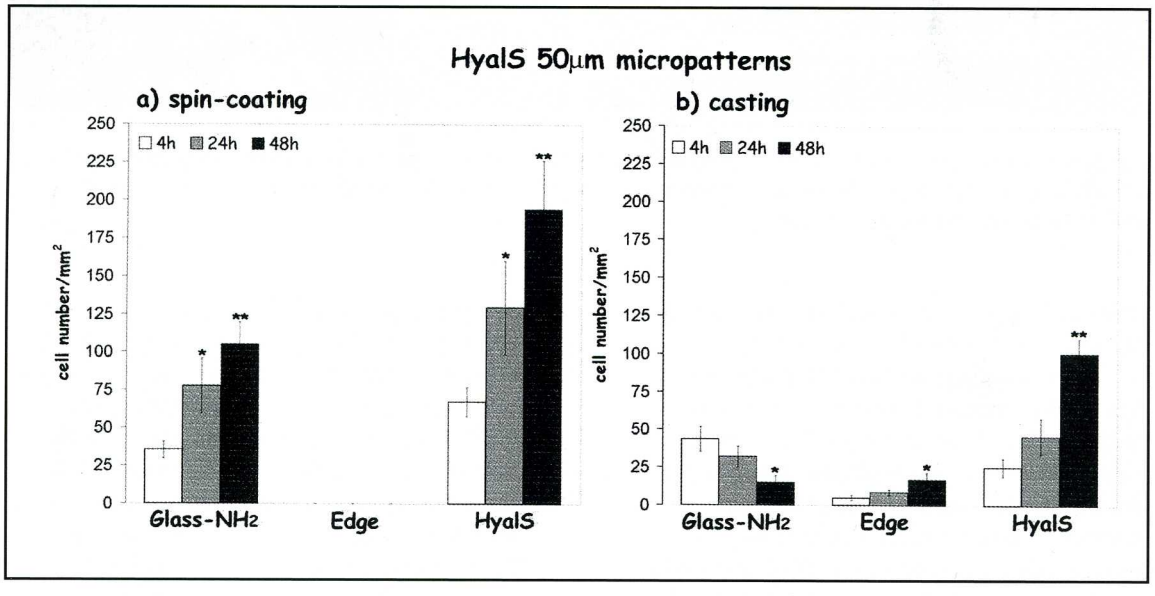

*Fig. 10. Cell number at 4, 24 and 48h on HyalS micropatterns of 50 μm obtained by a) spin-coating and b) casting. Counts were done on glass-NH_2 stripes, on HyalS stripes and on the edge between the two. Cell number was higher on micropatterns obtained by spin-coating at all times. On micropatterns obtained by casting, cell number at 48h decreased on glass-NH_2, increased on the edge and increased on HyalS. a) *P< 0.05 vs 4h, **P< 0.001 vs 4h, b) *P< 0.05 vs 4h, **P< 0.001 vs 4h and P< 0.005 vs 24h.*

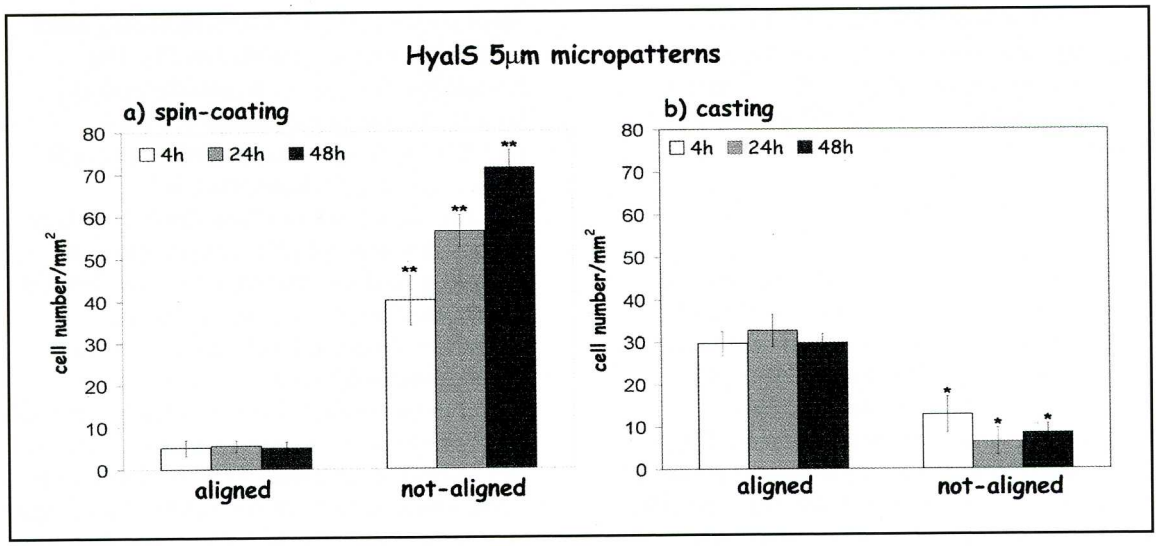

*Fig. 11. Alignment of LEC on HyalS micropatterns with 5μm wide stripes obtained by a) spin-coating and b) casting. At all times most cells aligned on micropatterns obtained by casting whereas the great majority of LEC seeded on micropatterns obtained by spin-coating did not align. a) **P< 0.001 vs aligned at the same time point, b) *P< 0.05 vs aligned at the same time point.*

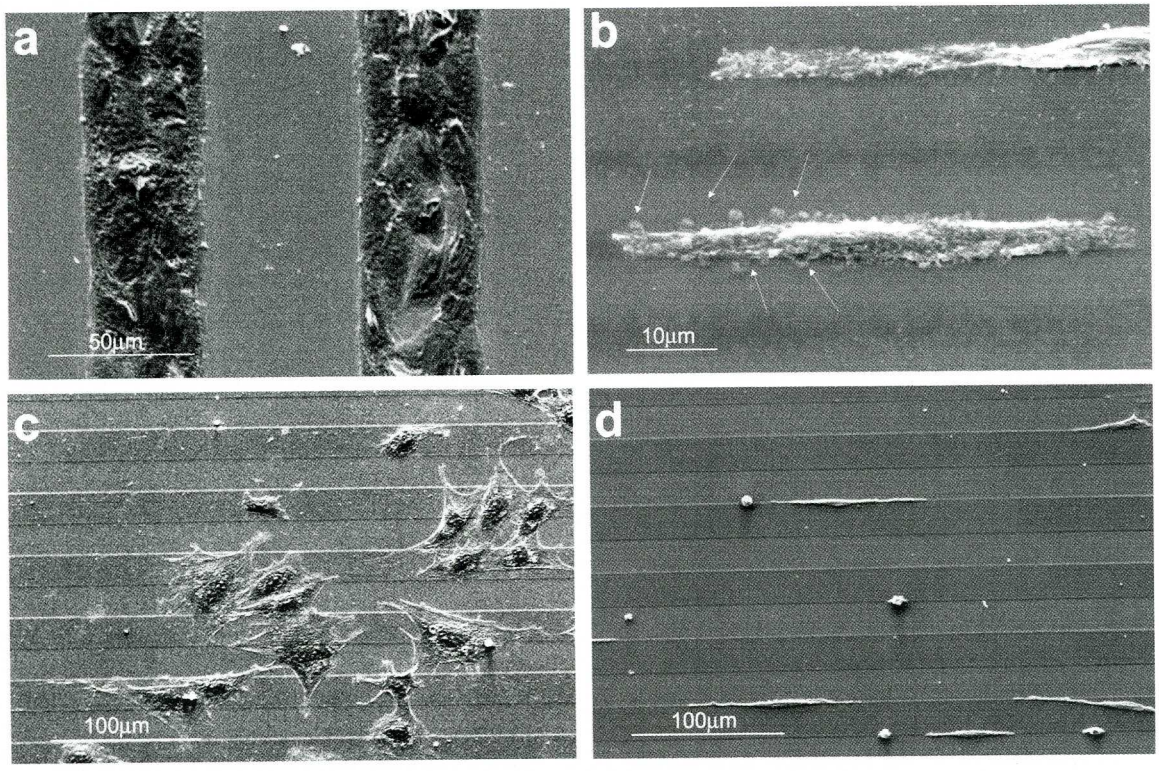

Fig 12. SEM micrographs showing cell adhesion on Hyal micropatterns with a) 50 and b) 5μm wide stripes and on HyalS micropatterns with 25μm wide stripes obtained by spin-coating c) and casting d). Arrows indicate pseudopodia.

proliferation limited by the narrowness of available space, whereas thinner stripes (obtained by spin-coating) were not detected, cells did not line up, and proliferation was favored.

SEM Analysis

SEM analysis of LEC cultured on Hyal micropatterns *(Fig. 12a and b)*, confirmed that cells lined up along substrate domains. On micropatterns with 5μm wide stripes *(Fig. 12b)*, several cells emitted small pseudopodia which apparently "sensed" the Hyal stripes edge. The narrowness of space available for spreading probably induced cells to attempt to expand in other directions.

On micropatterns of HyalS/glass-NH_2 with stripes of wide dimensions obtained by spin-coating *(Fig. 12c)*, cells randomly distributed on HyalS and glass-NH_2 with a spread flat morphology. On HyalS micropatterns obtained by casting, cells preferentially adhered to the polysaccharide domains; many cells aligned along the stripes' edge *(Fig. 12d)* with a polarized elongated shape.

DISCUSSION

The role of chemical cues in LEC behavior was investigated by the use of micropatterned surfaces with alternating stripes of Hyal/glass-NH_2 and HyalS/glass-NH_2. LEC consistently avoided Hyal stripes, as previously reported (4).

The reason why Hyal, which is one of the main components of the extracellular matrix, prevented cell adhesion may be the particular conformation assumed by the polysaccharide upon photoimmobilization (25). The covalent bond to the surface may decrease the degree of freedom of polymer chains hiding the suitable tridimensional organization necessary for cell-receptor interaction. It is known that CD44, a receptor highly selective for Hyal and present on the plasmatic membrane of several cell types including blood vessel endothelial cells, requires a polysaccharide oligomer with at least 6 or 8 repeating units to bind the polysaccharide (26,27). The homologue of CD44 in lymphatic endothelium is the lymphatic marker LYVE-1. LYVE-1 binds hyaluronan with apparently greater specificity than CD44. It is structurally related to CD44 (28,29), with an overall similarity of 43% and the greatest homology in the hyaluronan binding domains ("link" modules). We suggest that the interaction between Hyal and its receptor may become difficult when the polymer is bound to the surface forming a tridimensional network of several chains randomly oriented and assuming, as it does at physiological pH, a coil conformation. In this conformation, the minimum size (hexa- or octasaccharide units) required for receptor interaction becomes unavailable. The conformation assumed by HyalS at physiological pH, more stretched than Hyal for the presence of negatively charged sulphated groups, may conversely render its interaction with its receptor easier.

Integrins are known to mediate cell-substrate interactions. Integrin, FAK and actin distribution was evaluated in LEC cultured on Hyal/glass-NH_2 micropatterns to ascertain whether alignment affected their expression and orientation. The presence of integrins and FAK at the leading edge of migrating cells suggests that adhesion of cells to the surface is integrin-mediated and involves focal adhesion formation. Their co-localization suggests that signal transduction occurs from outside into the cell. It is known that FAK activation induces actin reorganization (30). Actin fibers indeed formed bundles parallel to the stripes in Hyal/glass-NH_2 micropatterns of all dimensions. The alignment of actin stress fibers in bundles parallel to the stripes demonstrates that cells adapt their shape to the micropattern geometry. Double staining showed that they terminated in correspondence of integrin dashes, apparently guided by them. HyalS promoted LEC adhesion and proliferation. We have previously reported (31) that in micropatterns obtained by laser ablation,

TABLE 1
Cell Adhesion to Hyal, HyalS and Glass-NH_2 Substrates

Cell type	Hyal	HyalS	Glass-NH_2
LEC	-	+	+
BAEC	-	+	+
HGTFN	-	+	-
3T3	-	-	+

HyalS promoted the adhesion of bovine aortic endothelial cells and prevented the adhesion of 3T3 fibroblasts. Cell adhesion and orientation on HyalS micropatterned surfaces seems therefore to be related to cell type. We here report that LEC adhere to HyalS just as bovine aortic endothelial cells. In this case, LEC and BAEC, which, in our experience, do not always respond similarly to the same stimulus (32), behaved similarly. The importance of testing the endothelial line of interest on a given surface is also highlighted by a previous work of some of us on the growth of an established endothelial cell line, HGTFN cells, on microstructured surfaces of HyalS/glass-NH_2. Interestingly, these cells avoided glass-NH_2 and aligned along the edge and on top of HyalS stripes. This behavior strongly resembles that of LEC on the Hyal/glass-NH_2 micropatterns used in this study. What is similar in the two different models is the alternation of stripes that promote cell adhesion and stripes that prevent it. In other words, alignment is obtained when cells are forced to avoid unfavorable chemical domains. In the same study, cell adhesion was also tested on microstructured surfaces of HyalS on a HyalS substrate. HyalS stripes were obtained in this case by photoimmobilization, in the presence of a photomask, of HyalS on a homogeneous, previously photoimmobilzed, HyalS layer. Under these conditions, in spite of the height of stripes, cells behaved as if they were on a homogeneous Hyal substrate equally spreading on the substrate and on top of HyalS stripes with random orientation. Topographical cues apparently did not affect the behavior of HGTFN cells. These data are summarized in *Table 1.*

The influence of topographical cues on LEC behavior was investigated here by varying micropattern dimensions (width, height). Alignment has been reported to be inversely proportional to features width and to correlate positively with groove depth (18,33-35).

We previously reported (4,24,36) that the Hyal micropatterns with thicker stripes (step height ~ 200-250nm) obtained by casting affect cell response and alignment exactly in the same way as the thinner striped surfaces obtained by spin-coating used in this work. Thus, in the case of Hyal micropatterns, cell alignment does not depend on the thickness of the polysaccharide tracks but rather on surface chemistry.

Stripe width proved also important in affecting cell behavior: 5μm wide stripes seemed to be the limit for endothelial cells to sense different adhesive and non-adhesive alternating domains and to line up. This limit probably depends also on cell dimensions; for example, the nucleus of LEC, which is not

dynamic and moldable as is the cytoplasm, has an average diameter of 6-8µm, just slightly bigger than the stripe width, so stripes are not large enough to accommodate the whole cell and part of it may fall over adjacent stripes. Two different behaviors were in fact observed for cells cultured on 5µm wide stripes: single prominent cells aligned along the pattern and colonies of cells with an elongated shape covering several adjacent stripes.

On HyalS micropatterns with thinner stripes (30-50nm) obtained by spin-coating, cells spread over the surface without any orientation, while on surfaces obtained by casting that had thicker stripes (200-250nm), cells reacted to the surface topography aligning on the stripe edge in all the micropatterns tested (50, 25 and 5µm). In the case of HyalS, the featured height thus plays a key role in affecting cell alignment. What attracts cells on the edge may be a merely topographical effect which becomes evident when the step is higher. HyalS micropatterns showed a sort of competition between the sulphated polysaccharide and glass-NH_2 towards cell adhesion. By extending time in culture, HyalS domains, however, attracted a larger number of cells than glass-NH_2.

In conclusion, Hyal micropatterns with a stripe pattern design have been shown to be a useful tool to guide LEC growth independently of the stripe step height, which indicates that surface chemistry affects LEC guidance more than surface topographical cues. When surface chemistry of stripes and substrate promotes cell adhesion as in the case of HyalS micropatterns, surface topography, in particular the height of the stripes, becomes the predominant factor responsible for LEC behavior. Hyal micropatterned surfaces are therefore preferable for LEC guidance and HyalS ones when adhesion is the priority. Much basic research is needed before a tissue-engineered strategy can be defined to overcome the great clinical challenge of lymphedema following surgical or traumatic interruption of lymphatic routes.

ACKNOWLEDGMENTS

The authors gratefully acknowledge the financial support of Fondazione Monte dei Paschi di Siena; University of Siena (PAR); Italian Ministry of Education University and Research (MIUR) for FIRB 2001 Project "Technologies for nanometric scale manufacture of materials and their biomedical application."

REFERENCES

1. Seifalian, AM, A Tiwari, G Hamilton, et al: Improving the clinical patency of prosthetic vascular and coronary bypass grafts: The role of seeding and tissue engineering. Artif. Organs 26 (2002), 307-320.
2. Shin'oka, T, Y Imai, Y Ikada: Transplantation of a tissue-engineered pulmonary artery. N. Eng. J. Med. 344 (2001), 532-533.
3. Matsumura, G, N Hibino, Y Ikada, et al: Successful application of tissue engineered vascular autografts: Clinical experience. Biomaterials 24 (2003), 2303-2308.
4. Weber, E, A Rossi, R Gerli, et al: Micropatterned hyaluronan surfaces promote lymphatic endothelial cell alignment and orient their growth. Lymphology 37 (2004), 15-21.
5. Band, PA: Hyaluronan derivatives: chemistry and clinical applications. In: the Chemistry, Biology and Medical Applications of Hyaluronan and its Derivatives. Laurent, TC (Ed.), Portland Press, London, 1998.
6. Bignami, A, R Asher: Some observations on the localization of hyaluronic acid in adult, newborn and embryonal rat brain. Int. J. Dev. Neurosci. 10 (1992), 45-57.
7. Fraser, JRE, TC Laurent: Hyaluronan. In : Extracellular Matrix. Comper, WD editor, Harwood Academic Publishers, Amsterdam 1996.
8. Knudson, CB, W Knudson: Hyaluronan-binding proteins in development, tissue homeostasis, and disease. FASEB J. 7 (1993), 1233-1241.
9. Toole, BP: Proteoglycans and hyaluronan in morphogenesis and differentiation. In: Cell Biology of Extracellular Matrix (Second edition), Hay, ED (Ed.), Plenum Press, New York, 1991.
10. Brecht, M, U Mayer, E Schlosser, et al: Increased hyaluronate synthesis is required for fibroblast detachment and mitosis. Biochem. J. 239 (1986), 445-450.

11. Toole, BP, C Biswas, J Gross: Hyaluronate and invasiveness of the rabbit V2 carcinoma. Proc. Natl. Acad. Sci. USA 76 (1979), 6299-6312.
12. Entwistle, J, CL Hall, EA Turley: HA receptors: Regulators of signalling to the cytoskeleton. J. Cell. Biochem. 61 (1996) 569-577.
13. Nakamura, H, S Kenmotsu, H Sakai: Localization of CD44, the hyaluronate receptor, on the plasma membrane of osteocytes and osteoclasts in rat tibiae. Cell Tissue Res. 280 (1995), 225-233.
14. Banerji, S, J Ni, S-X Wang, et al: LYVE-1, a new homologue of the CD44 glycoprotein, is a lymph-specific receptor for hyaluronan. J. Cell. Biol. 144 (1999), 789-801.
15. Magnani, A, A Albanese, S Lamponi, et al: Blood-interaction performance of differently sulphated hyaluronic acids. Thromb. Res. 81 (1996), 383-395.
16. Jeske, WP, AM Jay, S Hass, et al: Heparin-induced thrombocytopenic potential of GAG and non-GAG-based antithrombotic agents. Clin. Appl. Thromb. Hemost. 5 (1999), S56-62.
17. Clark, P, P Connolly, ASG Curtis, et al: Cell guidance by ultrafine topography in vitro. J. Cell. Sci. 99 (1991), 73-77.
18. Britland, S, H Morgan, B Wojiak-Stodart, et al: Synergistic and hierarchical adhesive and topographic guidance of BHK cells. Exp. Cell Res. 228 (1996), 313-325.
19. Magnani A, S Lamponi, R Rappuoli, et al: Sulphated hyaluronic acid : A chemical and biological characterisation. Polym. Int. 46 (1998), 225-240.
20. Chen GP, Y Ito, Y Imanishi: Photoimmobilization of sulfated hyaluronic acid for antithrombogenicity. Bioconjug. Chem. 8 (1997), 730-734.
21. Barbucci R, S Lamponi, A Magnani, et al: Micropatterned surfaces for the control of endothelial cell behaviour. Biomol. Eng. 19 (2002), 161-170.
22. Weber, E, P Lorenzoni, G Lozzi, et al: Culture of bovine thoracic duct endothelial cells. In Vitro Cell. Dev. Biol. 30A (1994), 287-288.
23. Voyta, JC, DP Via, CE Butterfield, et al: Identification and isolation of endothelial cells based on their increased uptake of acetylated-low density lipoprotein. J. Cell. Biol. 99 (1984), 2034-2040.
24. Barbucci, R, S Lamponi, A Magnani, et al: The use of Hyaluronan and its sulphated derivative patterned with micrometric scale on glass substrate in melanocytes cell behaviour. Biomaterials 24 (2003), 915-919.
25. Jackson, DG: Hyaluronan and lymphedema. Lymphology 37 (2004), 1-5.
26. Day, AJ, GD Prestwich: Hyaluronan binding proteins: Tying up the giant. J. Biol. Chem. 277 (2002), 4585-4588.
27. Knudson, W, CB Knudson: The Hyaluronan receptor CD44. http://www.glycoforum.gr.jp/science/hyaluronan/HA10/HA10E.html
28. Jackson, DG: Biology of the lymphatic marker LYVE-1 and applications in research into lymphatic trafficking and lymphoangiogenesis. APMIS 112 (2004), 526-538.
29. Prevo, R, S Banerji, DJP Ferguson, et al: Mouse LYVE-1 is an endocytic receptor for hyaluronan in lymphatic endothelium. J. Biol. Chem. 22 (2001), 19420-19430.
30. Burridge, K, CE Turner, LH Romer: Tyrosine phosphorylation of paxillin and pp125 FAK accompanies cell adhesion to extracellular matrix: a role in cytoskeletal assembly. J. Cell Biol. 119, (1992), 893-903.
31. Barbucci, R, S Lamponi, D Pasqui, et al: Micropatterned polysaccharide surfaces via laser ablation for cell guidance. Mat. Sci. Eng. C 23 (2003), 329-335.
32. Weber, E, P Lorenzoni, N Raffaelli, et al: Glioma cells induce (γ-glutamyl transpeptidase activity in cultured blood but not lymphatic endothelial cells. Biochem. Biophys. Res. Commun. 225, (1996), 1040-1044.
33. Brunette, DM: Fibroblasts on micromachined substrata orient hierarchically to grooves of different dimensions. Exp. Cell Res. 164 (1986), 11-26.
34. Clark, P, P Connolly, ASG Curtis, et al: Topographical control of cell behaviour: II. Multiple grooved substrata. Development 108 (1990), 439-448.
35. Dunn, GA, AF Brown: Alignment of fibroblasts on grooved surfaces described by a simple geometric transformation. J. Cell Sci. 83 (1986), 313-340.
36. Magnani, A, A Priamo, D Pasqui, et al: Cell behaviour on chemically microstructured surfaces. Mat. Sci. Eng. C 23 (2003), 315-328.

Prof. Elisabetta Weber, M.D.
Dipartimento di Neuroscienze
Sezione di Medicina Molecolare
University of Siena
Via Aldo Moro
53100 Siena, Italy
tel.: 0039 577 234083
fax: 0039 577 234191
e mail: weber@unisi.it